

Resistivity And Grain Size Dependent Magnetolectric Effect In (Y) $\text{Ni}_{0.85}\text{Cd}_{0.1}\text{Cu}_{0.05}\text{Fe}_2\text{O}_4$ + (1-Y) BaTiO_3 ME Composites

P. B. Belavi, G. N. Chavan, L. R. Naik, V. L. Mathe, R. K. Kotnala

Abstract: The Magnetolectric (ME) composites with composition (y) $\text{Ni}_{0.85}\text{Cd}_{0.1}\text{Cu}_{0.05}\text{Fe}_2\text{O}_4$ + (1-y) BaTiO_3 , (0.0 < y < 1.0) were synthesized by conventional solid state reaction method. The presence of constituent phases was confirmed by X-ray diffraction studies. Scanning electron microscopy was used to study the surface morphology of the composites. The average grain sizes were found to increase with ferrite content in the scanning electron micrographs of the composites. The percentage of constituent phases in the composites was rechecked and confirmed by EDX measurements. The decrease in dc resistivity with increase in temperature indicates semiconducting nature of the composites. The magnetic properties of the composites such as saturation magnetization and magnetic moment studied using vibration sample magnetometer are found to increase with ferrite content and are in agreement with theoretical values but magnetic transition temperature was found to decrease with ferrite content. However, the saturation polarization and remnant polarizations are found to decrease with increase of frequency as well as ferrite content in the composites. The maximum ME conversion factor of 16.8 mV/cm.Oe was observed for the composites with 15 mole % of ferrite and 85 mole % ferroelectric in the composites. High resistivity and low grain size of the composite exhibits high ME response at the same time these composites exhibits good multiferroic and magnetolectric properties with ferrite content. These ME composites are suitable for preparing flexible ME devices in electronics industries.

Index Terms: Composites, XRD, microstructure, EDX, Multiferroic, Magnetic moment, ME conversion factor.

1 INTRODUCTION

The ME composites are the special class of materials find wide applications in electrical and electronic industries. ME composites are used to design multifunctional devices in the field of sensors, magnetic storage device, transducers and actuators [1-5]. The ME composites can also be used in various fields such as microwave field, current measurements, integral optics and fiber communication technologies [6,7]. Infact, the coexistence of ferromagnetic and ferroelectric materials are known to exhibit magnetolectric effect at room temperature and play an important role in functioning of the composite material. Most of the composite materials are developed to improve mechanical properties viz, strength, stiffness and toughness etc. The ferrites and ferroelectrics are widely used in the preparation of ME composites as the interaction between these two subsystems give rise to ME effect and their strength of interaction is measured in terms of ME voltage coefficient. For the last few decades, intensive investigation on the perovskite BaTiO_3 (BTO) material is going on due to its excellent ferroelectric, dielectric, piezoelectric, pyroelectric, electro-optic and second harmonic properties as well as its lead-free and simple composition characteristics [8, 9].

Ferroelectrics are the most stable materials which have spontaneous polarization and can be switched hysteretically by applying an electric field. The ferroelectric material BaTiO_3 shows lower dielectric constant due to smaller grain size and substrate clamping effect. The ME coupling behavior of the material was used to generate electric polarization when it is placed in magnetic field and magnetization when it placed in electric field [10]. ME coefficient of composites mainly depends on the equilibrium between the two phases (ferromagnetic and ferroelectric) therefore it is essential to study dc resistivity and magnetic properties of the composites. The proper choice of ferrite and ferroelectric materials mainly depends on the magnetostriction coefficient, high piezoelectric coupling constant, high dielectric permittivity and high poling strength [11]. The structural, electrical, dielectric and magnetic properties of Ni ferrite doped with divalent metal ions such as Cu^{+2} , Zn^{+2} , Cd^{+2} , Co^{+2} and Mn^{+2} have been investigated by many researchers as these ferrites have high saturation magnetization, high stability and low dielectric loss at high frequency region and have microwave applications in electronics, humidity sensors, thermojunctions etc [11-15]. But Ni-Cu ferrite doped with Cd has not been studied so far. Infact, the Ni-Cu ferrite doped with Cd the Jahn-Teller ion Cu^{+2} with high coupling coefficient contributes more to the magnetostriction and that made us to study about these ferrites. Several researchers reported structural, electrical, dielectric and magnetic properties of the composites like NF+BTO [5], NCCF + BTO [14], NCF+BST [15], and NZF+BST [16] but not about Ni-Cd-Cu + BaTiO_3 composites. In the present work the ME composites of our interest was synthesized by using conventional solid state reaction method and their structural, electrical, magnetic and magnetolectric properties were studied including the effect of resistivity and grain size on ME effect. These ME composites are expected to exhibit good multiferroic and magnetolectric properties.

- Department of Studies in Physics, Karnatak University, Dharwad – 580 003, India, Email: naik_36@rediffmail.com
- Novel Materials Research Laboratory, Department of Physics, University of Pune – 411 007 (M S), India
- National Physical Laboratory, New Delhi – 110 012, India

2 EXPERIMENTAL

The ME composites with composition $(y) \text{Ni}_{0.85}\text{Cd}_{0.1}\text{Cu}_{0.05}\text{Fe}_2\text{O}_4 + (1-y) \text{BaTiO}_3$, $(0.0 < y < 1.0)$ were synthesized by conventional solid state reaction method. This method is easier as well as cheaper in fabrication and the grain size and sintering temperature can be easily controlled [17]. The AR grade NiO, CdO, CuO and Fe_2O_3 powders were taken as starting materials. Stoichiometric proportions of these materials were used to synthesize cadmium substituted nickel copper ferrite with the composition $\text{Ni}_{0.85}\text{Cd}_{0.1}\text{Cu}_{0.05}\text{Fe}_2\text{O}_4$ by conventional solid state reaction method. AR grade BaCO_3 and TiO_2 powders in molar proportions were used to synthesize the ferroelectric phase BaTiO_3 by using the same method. There after ferrite and ferroelectric powders were presintered at 800°C for 8 hrs. Afterwards the composites were prepared by mixing 15, 30 and 45 mole % of ferrite phase with 85, 70 and 55 mole % of ferroelectric phase respectively and presintered at 800°C for 8 hrs. Later on 2% of polyvinyl alcohol was added as a binder and pressed into disks of 10 mm in diameter and 2-3 mm in thickness using a pressure of 6-7 ton/sq.inch for 5 min. The pellets of composites and constituent phases were finally sintered at 1150°C for 12 hrs. The samples were characterized by X-ray diffraction technique to confirm the presence of constituent phases in the composites using Philips Model PW-1710 X-ray diffraction (XRD) with $\text{Cu-K}\alpha$ radiation ($\lambda = 1.5405 \text{ \AA}$). Surface morphologies of the composites were studied using scanning electron microscopy. The surface grain distribution and compositional features were carried out by using scanning electron microscopy (ESEM Quanta 200, FEI) equipped with energy dispersive X-ray spectroscopy (EDX). The temperature dependence dc resistivity of these samples were carried out using two probe method by silver pasting to well polished surfaces for good electrical conduction. The ferromagnetic hysteresis loop with temperature dependence magnetization of the composites were carried out by using vibrating sample magnetometer (VSM model 735, LakeShore) and the saturation magnetization (M_s), magnetic moment (μ_B) and magnetic transition temperature (T_c) was estimated. The magnetic moment (in Bohr magneton) of the composites was estimated using the relation given in ref [18]. The theoretical values of saturation magnetization were estimated using the sum rule given in ref[19], The ferroelectric P-E loops of the composites at two different frequencies (50 and 200 Hz) at room temperature were characterized by Radiant Technologies Ferroelectric Loop Tracer (*Precision Premier II Model*) interfaced with computer and was used to measure the saturation polarization and remnant polarizations. The proper electric and magnetic poling were made for the estimation of static ME voltage coefficient. For electric poling, the samples were heated about $20 - 30^\circ\text{C}$ above the ferroelectric Curie temperature (T_c) and cooled to room temperature under the influence of an external electric field of $2 - 2.5 \text{ KV/cm}$. These electrically poled samples were poled magnetically by applying a dc magnetic field of about 4.2 KOe at room temperature. The magnetic poling was done by placing the sample pellets inside the laboratory made sample holders with keeping it between the poles of a dc electromagnet. During the poling process the stray charges developed were eliminated by grounding the pellet holding plates. The static ME voltage coefficient was measured as a function of dc magnetic field. However, dc magnetic field was applied perpendicular to the polished and flat surfaces of the pellets and parallel to the direction of

applied electric field. The electric fields generated across the sample under the influence of dc magnetic field were measured by using Keithley electrometer (model 2000).

3 RESULTS AND DISCUSSION

Figure 1 (a) shows the X-ray diffraction pattern of the ferrite phase. All the peaks in the diffraction pattern are indexed, the prominent peak (3 1 1), confirms the cubic spinel structure of ferrite phase with lattice parameter $a = 8.364 \text{ \AA}$.

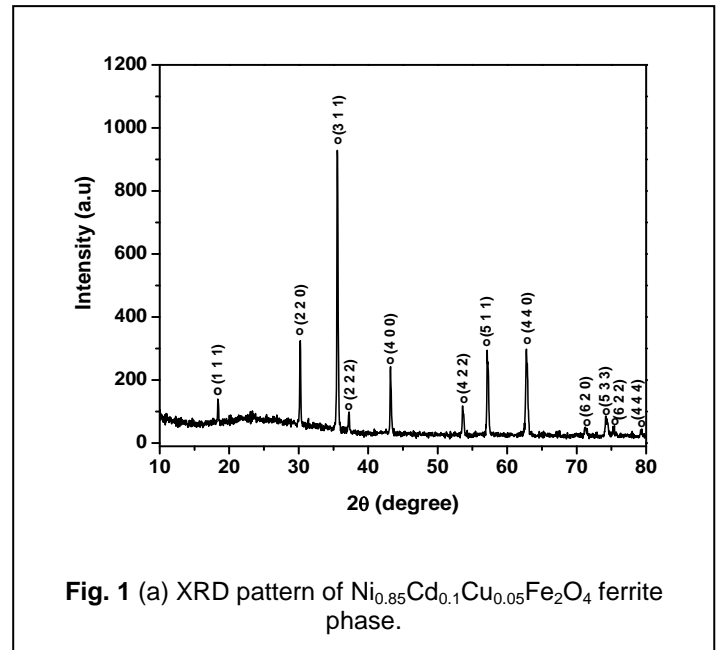


Fig. 1 (a) XRD pattern of $\text{Ni}_{0.85}\text{Cd}_{0.1}\text{Cu}_{0.05}\text{Fe}_2\text{O}_4$ ferrite phase.

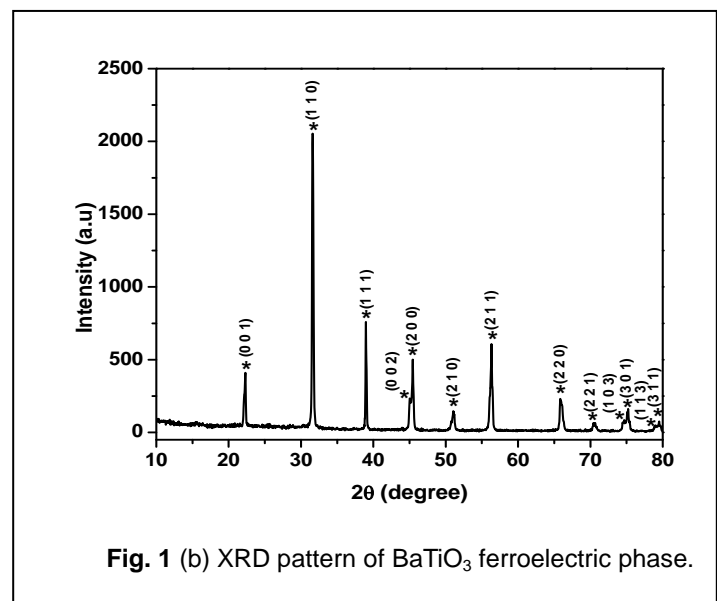
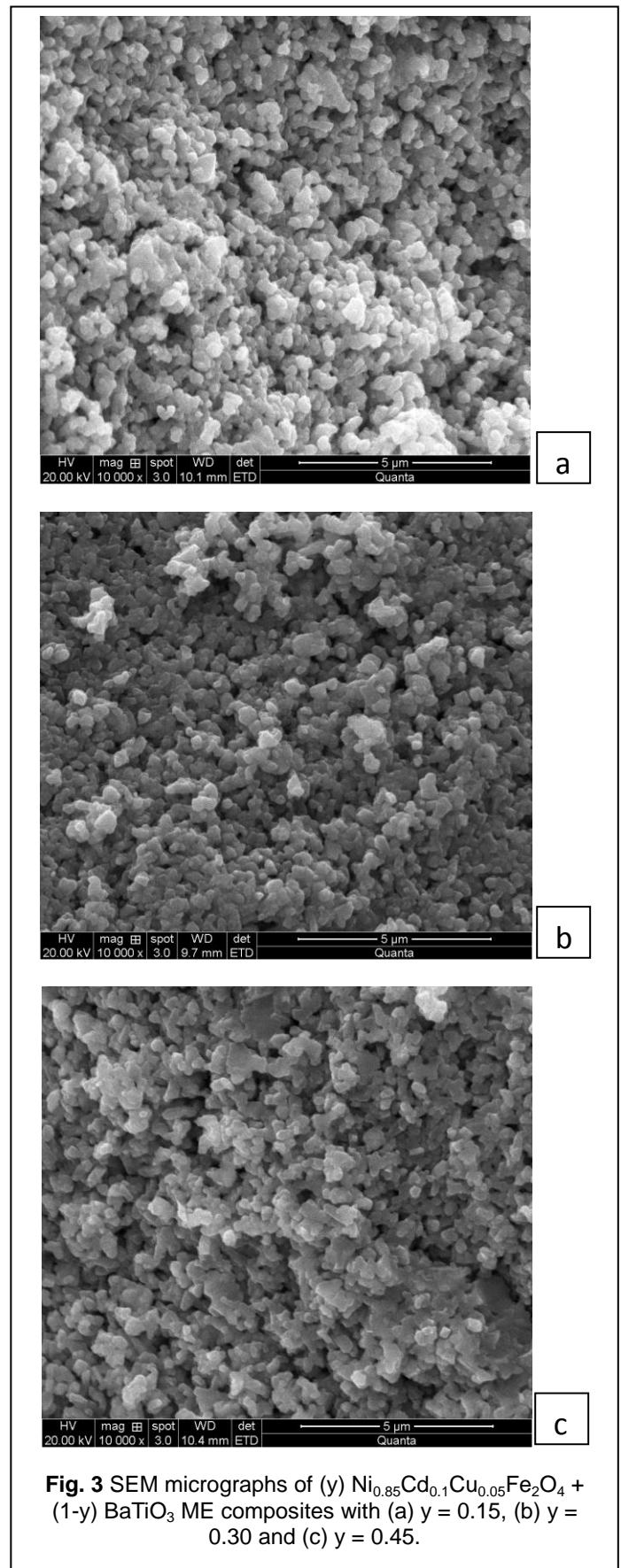
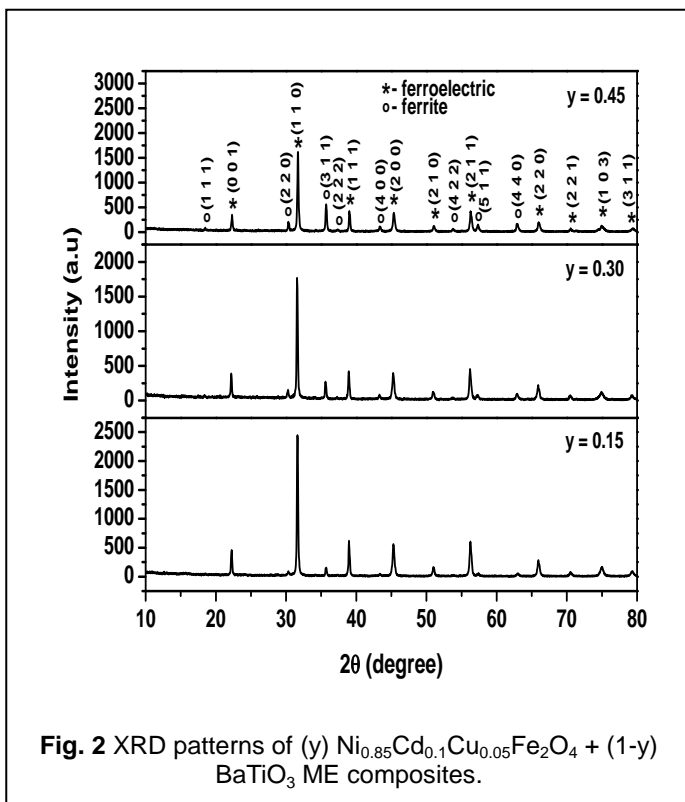


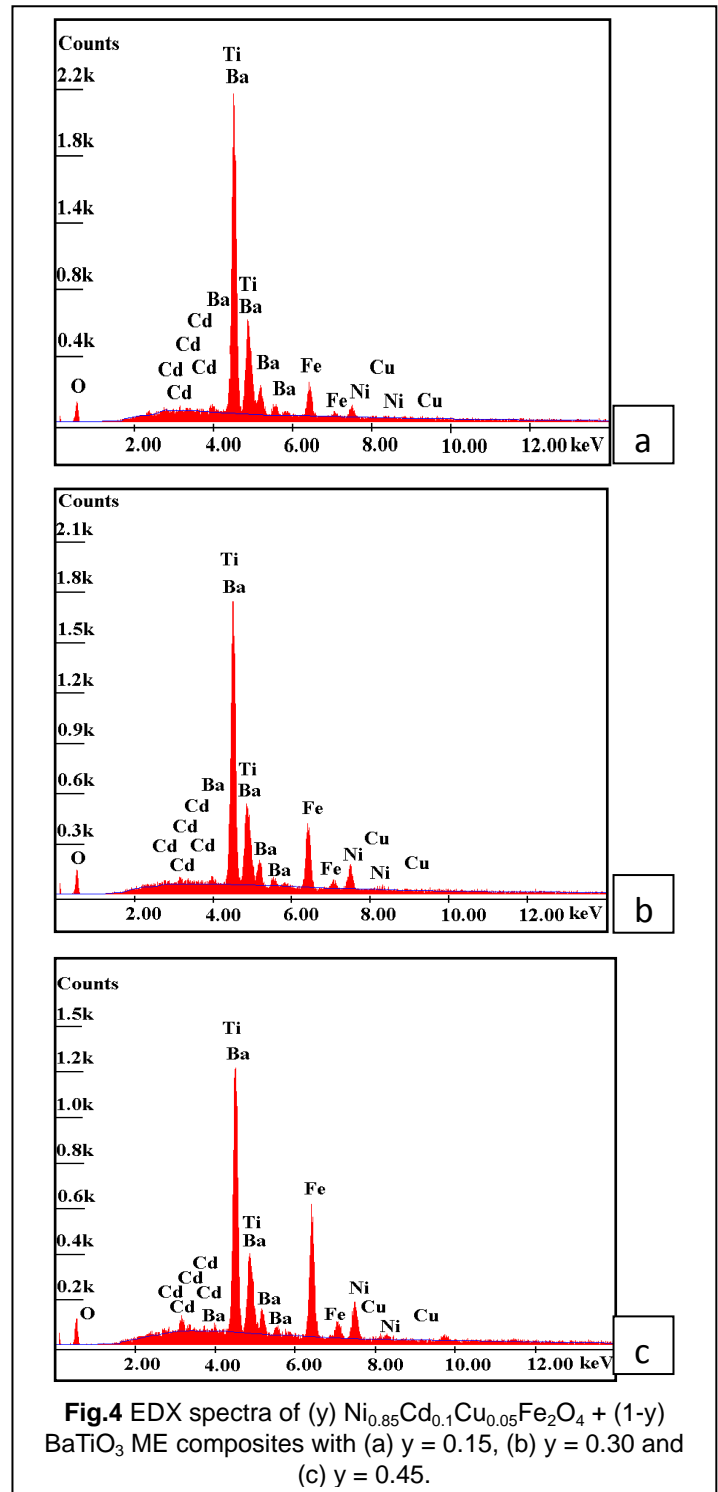
Fig. 1 (b) XRD pattern of BaTiO_3 ferroelectric phase.

The absence of extra peaks in the diffraction pattern suggests that no chemical reaction has occurred during the final sintering. All the doublet peaks appeared in the diffraction pattern of ferroelectric phase i.e. $(0 0 2) / (2 0 0)$, $(1 0 3) / (3 0 1)$ and $(1 1 3) / (3 1 1)$ as shown in figure 1 (b) are indexed and formation of tetragonal perovskite structure of ferroelectric phase were confirmed. The lattice parameters of ferroelectric phase estimated for the prominent peak (1 1 0) are found to

be $a = 3.999 \text{ \AA}$, $c = 4.000 \text{ \AA}$ (i.e. $c/a = 1.0002$). Figure 2 shows the X-ray diffraction pattern of composites with ferrite content. In the diffraction pattern of the composites the peaks corresponding to ferrite and ferroelectric phases are indexed from their individual XRD patterns. The appearance of two sets of well defined diffraction peaks in the diffraction patterns of composites confirms the cubic spinel structure of ferrite phase and tetragonal perovskite structure of ferroelectric phase in the composites. The estimated lattice parameters of the composites listed in Table 1 are almost equal to its constituent phases. The non variation of the tetragonal ratio (i.e. $c/a = \text{constant}$), indicates non structural variations with mol % of ferrite and ferroelectric phases in the composites. The slight variation in lattice parameters with mol % of ferrite phase was due to the difference in the ionic radii of the component ions. The Cd^{+2} ions have larger ionic radius (0.097 nm) than Cu^{+2} (0.073 nm), Ni^{+2} (0.069 nm) and Fe^{+3} (0.0645 nm) ions [19]. However, the number of diffraction peaks with intensity depends on the mol % of constituent phases in the composites. The increase in the intensity of (3 1 1) peak in ferrite phase and decrease in the intensity of (1 1 0) peak in ferroelectric phase was observed as a function of the increase in ferrite content of composites.

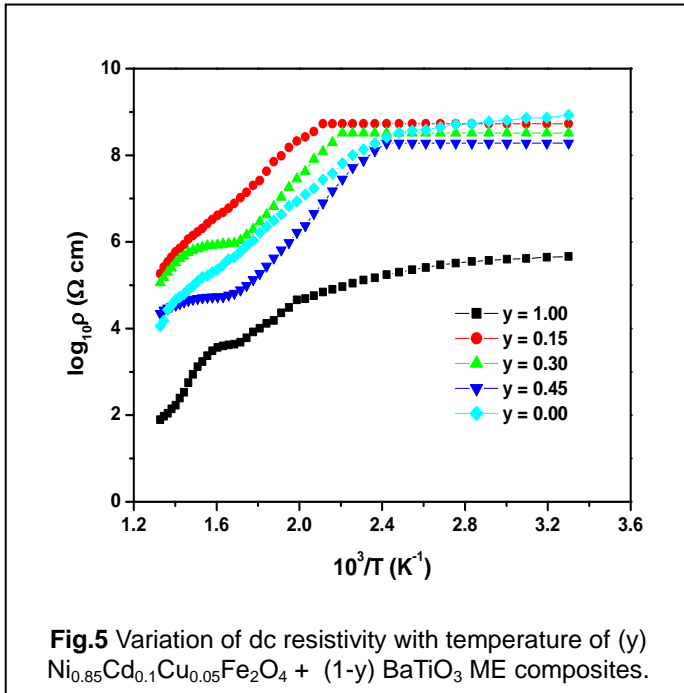


The average grain sizes of the composites estimated by Cottrell's method [20] were found to increase with ferrite contents and are less than the pure ferroelectric phase (Table 1). The XRD patterns and SEM micrographs of composites suggests non- inter diffusion between the phases during the final stage of the sintering. The increase of average grain size of the composites with decrease in porosity decreases the grain boundary area and acts as an obstacle for domain wall motion. The increase of average grain size with ferrite content results in the increase of mean free path of electron and causes the increase of resistivity and ME response in the composites. The presence of pores in the samples breaks the magnetic circuit between the grains; in the present composites the decrease in porosity with ferrite content increases the net magnetization as the resistance of the magnetization with increased grain size makes magnetization to increase more easily. Figure 4 (a-c) shows the energy dispersive X-ray spectrum (EDX) of composites with different ferrite contents. The non-observation of elements other than Ni, Cd, Cu, Fe, O, Ba and Ti in the EDX spectra reveals the absence of chemical reaction during final sintering, which confirms the formation of biphases of cubical spinal structure of ferrite and tetragonal perovskite structure of ferroelectric phase in the composites. Systematic variation in the intensities of ferrites and ferroelectrics were observed. The peak intensity of ferrite phase increases with ferrite content (i.e. Ni, Fe, Cd and Cu), where as the peak intensity of ferroelectric phase (i.e. Ba and Ti) decreases. The percentage compositions of constituent phases after final sintering were estimated from the EDX measurements and are tabulated in Table 2. It is to be noted that the expected values of percentage composition of constituent phases in the composites and the values obtained from EDX measurements are in good agreement. Electrical resistivity is an important property for the study of ME effect as the study of electrical resistivity gives valuable information about the behavior of free and localized electric charge carriers in the samples. In order to get high magnetoelectric effect, resistivity of the composites should be high and there must not be leakage of accumulated charge carriers through the magnetostriction phase. The variation of dc resistivity of composites with temperature is shown in Fig. 5. The figure shows the two region of conductivity, the first region of conductivity observed at lower temperature was due to the impurities and is attributed to order state of ferroelectric phase and the second region of conductivity observed at higher temperature is due to polaron hopping and is attributed to disordered paraelectric phase of composites [21]. However, the impurities present in the system are almost minimized and polaron hopping type of conduction mechanism is valid in ferroelectric as well as in composites at higher temperature [22]. The resistivity of the composites goes on increases and almost constant up to certain temperature and there after it decreases. All the samples show the semiconducting nature with increasing temperature. According to hopping conduction mechanism the decrease in resistivity with increase in temperature was due to the increase in thermally activated drift mobility of charge carriers.

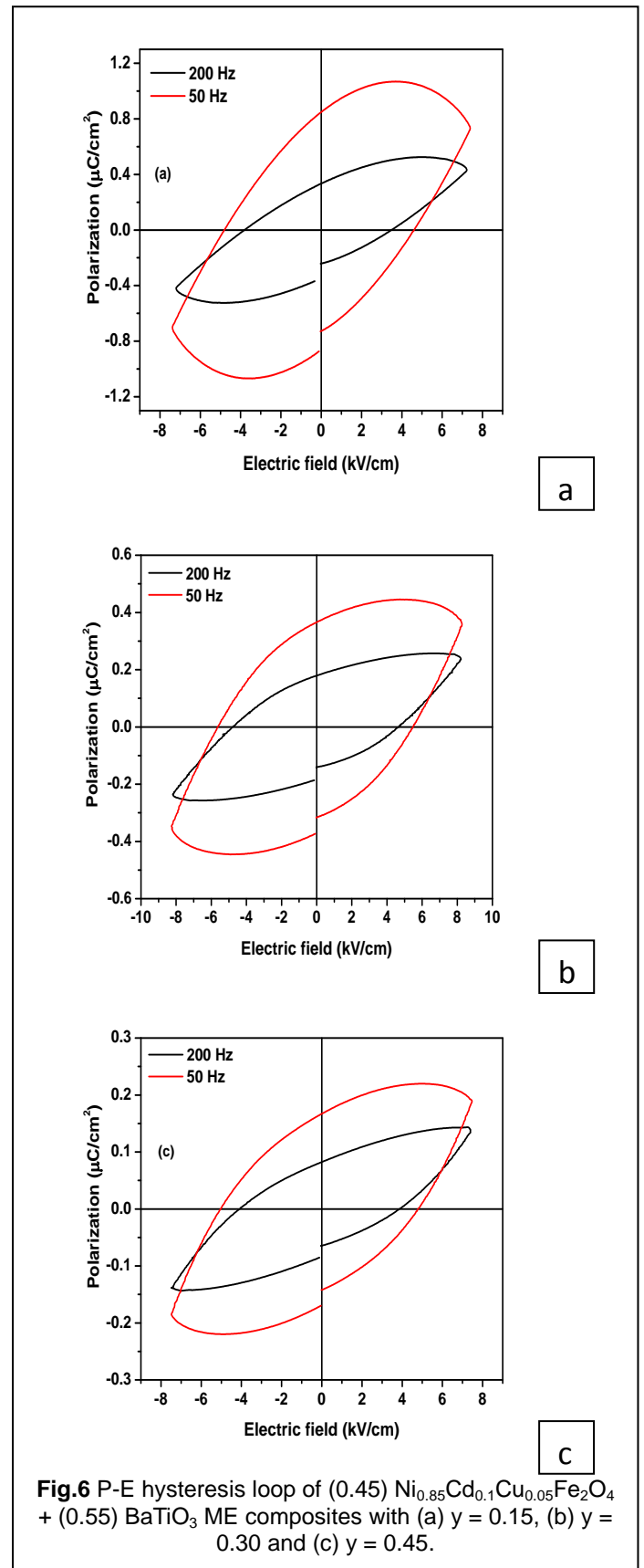


The resistivity of the ME composites are found to decrease with increase in ferrite content. If the ferrite particles are dispersed throughout the composites and if they make the chains with ferroelectric particles then electrical conductivity of the composites reduces significantly. The conduction mechanism in ferrites were explained on the basis of Verwey and DeBoer [23] mechanism, which involves the exchange of electrons between the ions of the same elements as they are randomly distributed over the crystallographic equivalent lattice sites. The exchange of electron between $\text{Fe}^{2+} \leftrightarrow \text{Fe}^{3+} +$

e^- , $Ti^{3+} \leftrightarrow Ti^{4+} + e^-$ is responsible for n-type charge carriers and the exchange of hole between $Ni^{3+} \leftrightarrow Ni^{2+} + e^+$, $Cu^{2+} \leftrightarrow Cu^{1+} + e^+$, $Cd^{2+} \leftrightarrow Cd^{1+} + e^+$ and $Ba^{3+} \leftrightarrow Ba^{2+} + e^+$ is responsible for p-type charge carriers and are responsible for electrical conduction in the composites [19]. The number of such ions depends upon the sintering condition and amount of reduction of Fe^{2+} to Fe^{3+} ions at elevated firing temperature.



The ferroelectric hysteresis loops of the composites at room temperature are shown in Fig. 6 (a-c). Similar behavior of the ferromagnetic hysteresis loop and ferroelectric hysteresis loops of the composites were observed. Higher ferrite content in the composites results in the lower polarization values. From the Fig. 6 (a-c) we notice that the polarization decreases with increasing frequency, it is due to capacitance effect at a high frequency [24]. The ferrite phase mixed in to ferroelectric phase acts as pores in the presence of applied electric field and breaks the electric circuit, resulting in the decrease of ferroelectric parameters i.e. saturation polarization and remnant polarization with increasing the ferrite concentration. The saturation polarization and remnant polarization of the composites increase with ferroelectric content and the individual ferroelectric grains acts as centre of polarization, the saturation polarization of the composites is the vector sum of all these individual contribution. Figure 7 shows the magnetic hysteresis loops of the composites at room temperature. All the composites exhibit typical magnetic hysteresis loop indicating the presence of an ordered magnetic structure in the mixed cubic spinel structure of ferrite phase and tetragonal perovskite structure of ferroelectric phases in the composites. The magnetic hysteresis loops of the composites shift towards the field axis with decreasing ferrite content. The estimated saturation magnetization and magnetic moments are tabulated in Table 2.



The increase of saturation magnetization and magnetic moment was observed with ferrite content. It is because individual ferrite grains act as centers of magnetization and the

saturation magnetization of the composites is the vector sum of all these individual contributions.

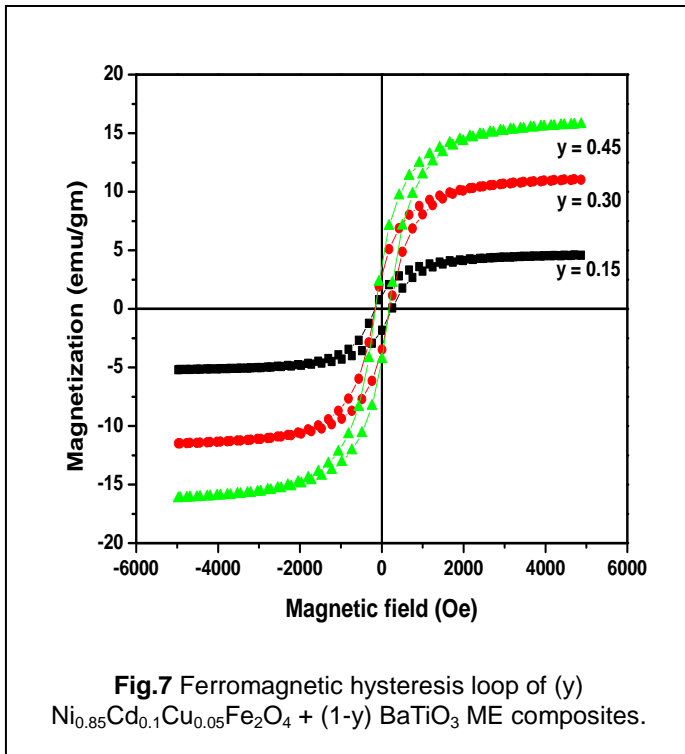
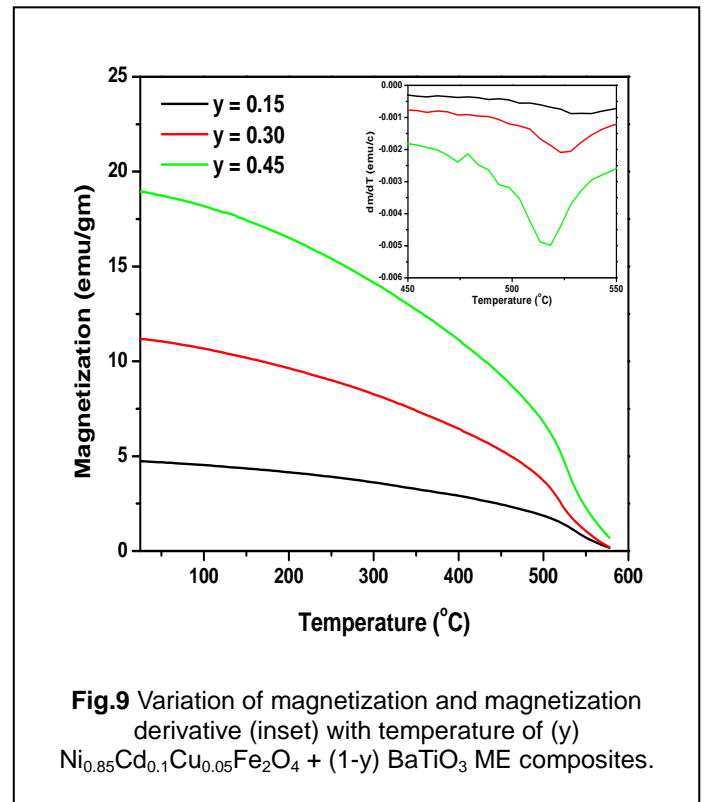
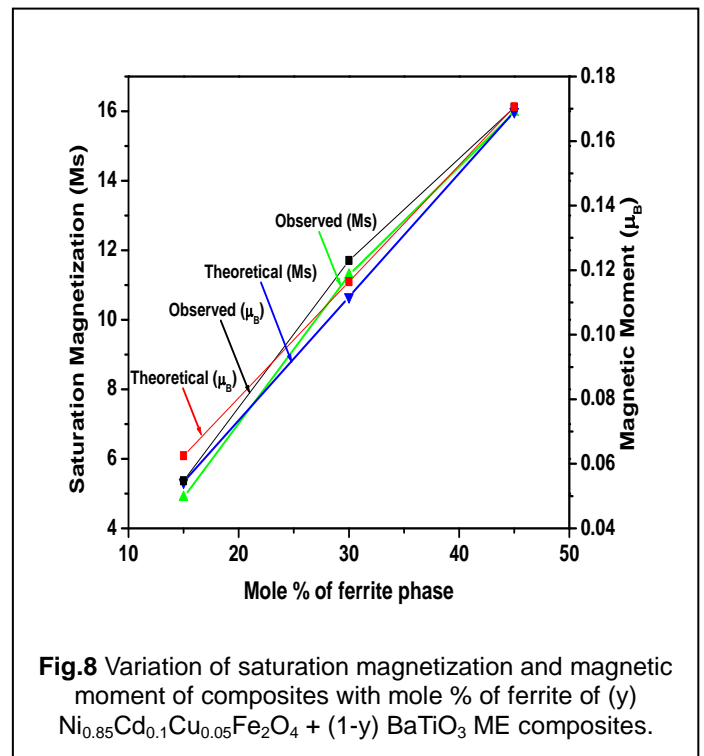


Figure 8 shows the variation of observed and theoretical saturation magnetization and magnetic moment with mole % of ferrite. From the figure it is to be noted that the observed and theoretical saturation magnetization and magnetic moments are in good agreement with each other. In the present composites, the average grain size increases and porosity decreases with increasing ferrite content, which affects the magnetic parameters. The saturation magnetization for the composites is less than that for pure ferrites (Table 2). This is because the presence of pores among the grains breaks the magnetic circuit between the grains and results in the decrease of magnetic parameters. That is the ferroelectric material added to the ferrite material, acts as pore in the presence of magnetic field and breaks the magnetic circuit, resulting in the decrease of magnetic parameters with increasing ferroelectric content in the composites [11]. The net increase in magnetization with decrease in porosity with increasing ferrite content affects the resistance of the magnetization and increases the grain size. Thus magnetization gets increased more easily and results in an increase of magnetic parameters i.e. saturation magnetization and magnetic moment. Figure 9 shows the temperature dependence of magnetization of composites with different ferrite content. From the figure it is clear that initially the magnetization is almost saturate and then slowly decreases with increasing temperature. At a particular temperature (T_c) the magnetization changes its slope, due to magnetic transition. The magnetic transition temperature (T_c) of the composites can be determined from the minimum position of the dM/dT versus temperature curve, shown in the inset of figure 9. The decrease in magnetic transition temperature (T_c) with increase of the ferrite content increases magnetization (Table 2).



The magnetoelectric conversion factor in composites having ferrite and ferroelectric phases depends on the applied magnetic field, electrical resistivity, mole % of constituent phases, mechanical coupling between the two phases and grain size [11]. According to product property (magnetoelectric effect) i.e. an applied magnetic field induces an electric field and vice-versa. When magnetic field is applied to the

composites the strain is generated in the ferrite phase and that strain induces stress on the ferroelectric phase. Thus magnetolectric voltage coefficient can be estimated by magnetomechanical conversion in the ferroelectric phase by stress transfer through the interface between two phases.

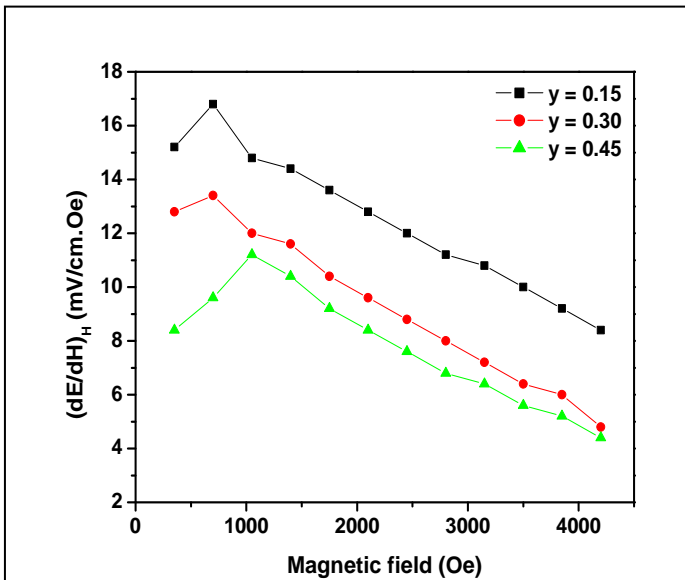


Fig.10 Magnetic field dependent variation of ME voltage coefficient for (y) $\text{Ni}_{0.85}\text{Cd}_{0.2}\text{Cu}_{0.05}\text{Fe}_2\text{O}_4 + (1-y) \text{BaTiO}_3$ ME composites.

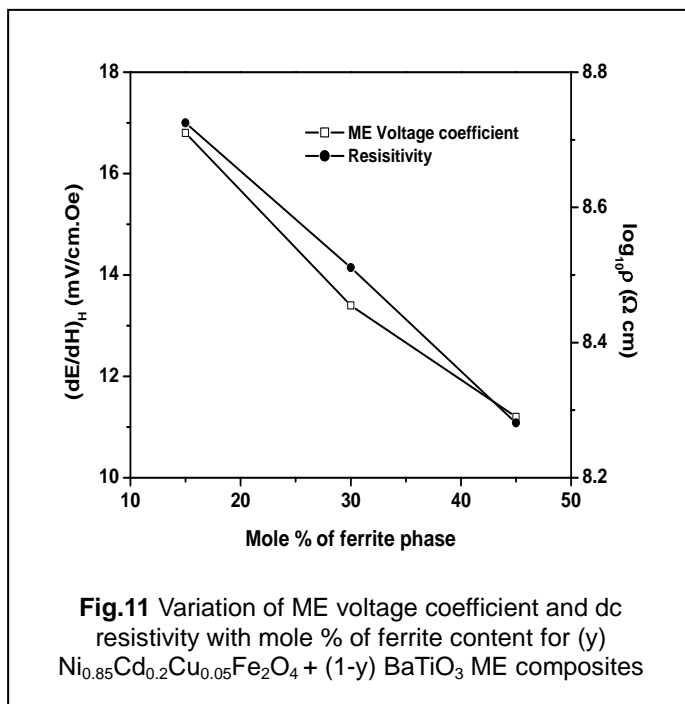


Fig.11 Variation of ME voltage coefficient and dc resistivity with mole % of ferrite content for (y) $\text{Ni}_{0.85}\text{Cd}_{0.2}\text{Cu}_{0.05}\text{Fe}_2\text{O}_4 + (1-y) \text{BaTiO}_3$ ME composites

The variation of magnetolectric voltage coefficient with applied dc magnetic field at room temperature for $y = 0.15, 0.30$ and 0.45 mole % of ferrite in composites as shown in Fig. 10. From the figure it is clear that the magnetolectric voltage coefficient increases gradually with magnetic field and attains

a maximum value, there after it decreases at higher magnetic field. The initial increase of magnetolectric voltage coefficient was due to the enhancement in elastic interaction and was confirmed by the hysteresis measurement. The maximum value of magnetolectric voltage coefficient indicates that the magnetostrictive phase reaches its saturation value at the time of magnetic poling and that produces constant electric field in the ferroelectric phase, forcing the magnetolectric voltage coefficient to decrease with increasing magnetic field [25]. The variation of magnetolectric voltage coefficient and dc resistivity with ferrite content is shown in Fig. 11. The magnetolectric voltage coefficient was found to be maximum for highly resistive composites. The magnetolectric voltage coefficient depends on mole % of constituent phases in the composites. The maximum magnetolectric voltage coefficient was observed for 15 mole % and minimum for 45 mole % of ferrite phase in the composites. The composites containing high ferrite phase cannot be poled at a high electric voltage as its resistance goes on decreases as mole % of ferrite phase increases as compared to ferroelectric phase and one cannot get high piezoelectric effect due to the leakage of charges developed in the ferroelectric grains through the path of the low resistance of the surrounding ferrite grains. This leakage of charges reduces the magnetolectric effect of the composites.

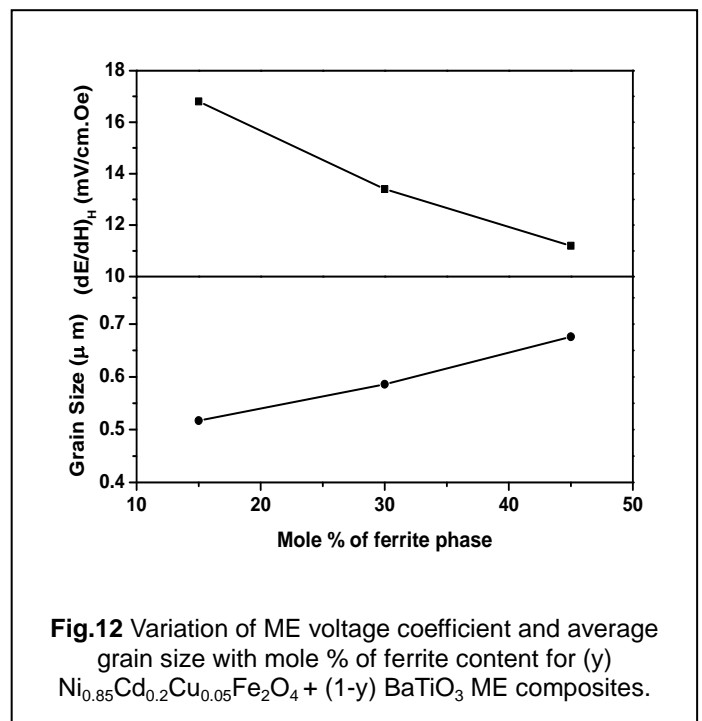


Fig.12 Variation of ME voltage coefficient and average grain size with mole % of ferrite content for (y) $\text{Ni}_{0.85}\text{Cd}_{0.2}\text{Cu}_{0.05}\text{Fe}_2\text{O}_4 + (1-y) \text{BaTiO}_3$ ME composites.

The variation of magnetolectric voltage coefficient and average grain size with ferrite content in the composites are shown in figure 12. From the Figure it is clear that the magnetolectric voltage coefficient decreases and grain size increases with increasing the ferrite content in the composites. The large grains are less effective in inducing piezomagnetic and piezoelectric coefficient than smaller ones [11]. Motagi and Hiskins reported the variation of piezoelectric property of ferroelectric phase with grain size [26]. In the present experimental results it is found that small grains plays an important role for getting the high magnetolectric (ME) output

in the composites.

TABLE 1: LATTICE PARAMETERS, POROSITY (P), AVERAGE GRAIN SIZE (D) OF COMPOSITES AND ITS CONSTITUENT PHASES

(y)	Lattice parameters (Å)				P (%)	D (µm)
	Ferrite		Ferroelectric			
	'a'	'a'	'c'	'c/a'		
0.00	-	3.999	4.000	1.0002	23.2	0.799
0.15	8.327	3.999	4.000	1.0002	22.7	0.517
0.30	8.347	4.003	4.004	1.0002	20.2	0.586
0.45	8.334	3.988	3.989	1.0002	18.7	0.676
1.00	8.364	-	-	-	14.4	1.466

TABLE 2.1: PERCENTAGE OF COMPOSITION

(y)	Percentage of composition (%)			
	Ferrite		Ferroelectric	
	Expected	EDX	Expected	EDX
0.15	15.00	14.63	85.00	85.36
0.30	30.00	29.85	70.00	70.14
0.45	45.00	44.17	55.00	55.82

TABLE 2.2: SATURATION MAGNETIZATION (MS), MAGNETIC MOMENT (µ_B), MAGNETIC TRANSITION TEMPERATURE (T_C) AND MAGNETIZATION (M) AT 25 °C OF COMPOSITES

(y)	Ms (emu/gm)	µ _B	T _C (°C)	M at 25 °C (emu/c)
0.15	4.888	0.054	528	4.732
0.30	11.288	0.123	523	11.175
0.45	15.969	0.170	518	18.961

4 CONCLUSION

The present ME composites were synthesized by standard double sintering ceramic method. The XRD pattern of the ME composites reveals the cubic spinel structure of ferrite phase and tetragonal perovskite structure of ferroelectric phase. The intensity of the (3 1 1) peak in ferrite phase increases while intensity of the (1 1 0) peak in ferroelectric phase decreases upon the increase of ferrite content in the composites. The average grain size in the composites increases with increase in ferrite content. The expected percentage of composition of composites compared with EDX measurements are in good agreement with each other. The saturation magnetization, magnetic moments are found to increase while magnetic transition temperatures was found to decrease with increases in ferrite content in the composites. The saturation and remnant polarization of the composites decreases with frequency as well as the ferrite content. All the composites exhibit the multiferroic (i.e. ferromagnetic and ferroelectric) in

nature. The highest ME conversion factor of 16.8 mV/cm.Oe was observed for the composites with 15 mole % of ferrite and 85 mole % of ferroelectric phases in the composites. The present ME composites are suitable for preparing flexible ME devices such as magnetoelectric memory, sensors, cables and also in electronics industries.

ACKNOWLEDGMENT

One of the author (LRN) is grateful to UGC, New Delhi, for sanctioning the major research project (F.No.34-34/2008 (SR) dated. 30/12/2008). The author (PBB) thanks to UGC, New Delhi, for award of research fellowship under RFSMS scheme and CSIR New Delhi for the award of SRF. Authors are thankful to Dr. V. R. Reddy, UGC-DAE, CSR, Indore (MP), for providing ferroelectric loop tracer experimental facilities.

REFERENCES

- [1] J.V. Suchetelene, *Philips Res Rep* 27, 28, 1972
- [2] G. Sreenivasulu, V.H. Babu, G. Markandeyulu, B.S. Murty, *Appl Phys Lett* 94, 112902, 2009
- [3] C.W. Nan, M.I. Bichurin, S. Dong, D. Viehland, G. Srinivasan, *J Appl Phys*, 103, 031101, 2008
- [4] M. Fiebig, *J Phys D* 38, R123, 2005
- [5] LP.M. Bracke, R.G.V. Vlient, *Int J Electronics* 51,255, 1981
- [6] B.K. Bammannavar, L.R. Naik, R.B. Pujar, B.K. Chougule, *J Alloys Compd* 477, L4, 2009
- [7] K. Uchino, *Piezoelectric Composites Chap.5.24 Comprehensive Composite Materials Elsevier Science, Oxford, UK* 2000
- [8] J.F. Scott, *Science* 315, 954, 2007
- [9] L. Qiao, X.F. Bi, *J Cryst Growth* 310, 2780, 2008
- [10] C.M. Kanamadi, B.K. Das, C.W. Kim, D.L. Kang, H.G. Cha, H.S. Ji, A.P. Jadhav, B.E. Jun, J.H. Jeong, B.C Choi, B.K. Chougule, Y.S. Kang, *Matt Chem Phys* 116, 6, 2009
- [11] B.K. Bammannavar, L.R. Naik, B.K. Chougule, *J Appl Phys* 104, 064123, 2008
- [12] A.M. Abdeen, *J Magn Magn Mater* 185, 199, 1998
- [13] O.H. Kwon, Y. Fukushima, M. Sugimoto, N. Hiratsuka, *J Phys IV*, 165, 1997
- [14] R.S. Devan, Y.D. Kolekar, B.K. Chougule, *J Alloys Compd* 461, 678, 2008
- [15] M.B. Shelar, P.A. Jadhav, B.K. Chougule, V.R. Puri, *Int J Self-Prop High Synth* 19(2), 102, 2010
- [16] H. Yang, H. Wang, L. He, L. Shui, X. Yao, *J Appl Phys* 108, 074105, 2010

- [17] P.B. Belavi, G.N. Chavan, L.R. Naik, R.K. Kotnala, *Inter J Nanosci* 11(3), 1240007, 2012
- [18] B.K. Bammannavar, L.R. Naik, *Smart Mater Struct.* 18, 085013, 2009
- [19] P.B. Belavi, G.N. Chavan, L.R. Naik, R. Somashekar R.K. Kotnala, *Mater Chem Phys* 132, 138, 2012
- [20] A. Cottrell, *An Introduction to Metallurgy* Edward Arnold Publishing Ltd, London 1967
- [21] R.P. Mahajan, K.K. Patankar, A.N. Patil, S.C. Choudhary, A.K. Ghatage, S.A. Patil, *J Eng Mater Sci* 7, 203, 2000
- [22] R.N.P. Choudhary, S.R. Shannigrahi, A.K. Singh, *Bull Mater Sci* 22(6), 75, 1999
- [23] E.J.W. Verwey, F.De. Boer, J.H. Vasanten, *J Chem Phys* 161, 1091, 1948
- [24] W. Chen, Z.H. Wang, W. Zhu, U.K. Tan, *J Phy D Appl Phys* 42, 075421, 2009
- [25] N. Cai, J. Zahi, C.W. Nan, Y. Lin, Z. Shi, *Phy Rev B* 68, 224103, 2003
- [26] H. Motagi, S. Hiskins, *Jpn J Phys Soc* 29, 524, 1970